Separation Science and Technology
Publication details, including instructions for authors and subscription information:
http://www.informaworld.com/smpp/title~content=t713708471

Studies Relating to Removal of Arsenate by Electrochemical Coagulation: Optimization, Kinetics, Coagulant Characterization

Subramanyan Vasudevan[a]; Jothinathan Lakshmi[a]; Ganapathy Sozhan[a]
[a] Central Electrochemical Research Institute (Council of Scientific and Industrial Research), Karaikudi, India

Online publication date: 02 June 2010

To cite this Article Vasudevan, Subramanyan , Lakshmi, Jothinathan and Sozhan, Ganapathy(2010) 'Studies Relating to Removal of Arsenate by Electrochemical Coagulation: Optimization, Kinetics, Coagulant Characterization', Separation Science and Technology, 45: 9, 1313 — 1325
To link to this Article: DOI: 10.1080/01496391003775949
URL: http://dx.doi.org/10.1080/01496391003775949

Separation Science and Technology, 45: 1313–1325, 2010

ISSN: 0149-6395 print/1520-5754 online
DOI: 10.1080/01496391003775949

Taylor & Francis
Taylor & Francis Group

Studies Relating to Removal of Arsenate by Electrochemical Coagulation: Optimization, Kinetics, Coagulant Characterization

Subramanyan Vasudevan, Jothinathan Lakshmi, and Ganapathy Sozhan
Central Electrochemical Research Institute (Council of Scientific and Industrial Research), Karaikudi, India

The present investigation aims to remove arsenate [As(V)] by electrochemical coagulation using mild steel as anode and cathode. The results showed that the optimum removal efficiency of 98.6% was achieved at a current density of 0.2 A dm^{-2}, at a pH of 7.0. The effect of current density, solution pH, temperature, co-existing ions, adsorption isotherm, and kinetics has been studied. Kinetics reveals that the removal of arsenate by electrochemical coagulation is very rapid in the first 15 min and remains almost constant with the progress of reaction. The adsorption kinetics obeys the second-order rate expression. An equilibrium isotherm was measured experimentally and the results were analyzed by Langmuir, Freundlich, Dubinin- Redushkevich, and Frumkin using the linearized correlation co-efficient. The characteristics parameters for each isotherm were determined. The Langmuir adsorption isotherm was found to fit the equilibrium data for arsenate adsorption. Temperature studies showed that the adsorption was endothermic and spontaneous in nature.

Keywords adsorption kinetics; arsenate removal; electrochemical coagulation; isotherms

INTRODUCTION

Arsenic, which is toxic to man and other living organisms, presents potentially serious environmental problems throughout the world. Unfortunately, there is no known cure for arsenic poisoning and therefore providing arsenic free drinking water is the only way to diminish the adverse health affects of arsenic. Arsenic is an environmental health concern, because long-term epidemiological studies demonstrate that it is toxic to humans and other living organisms. Arsenic from natural and manmade sources has gotten into many water sources, especially well water sources. The other sources of arsenic are metallurgical industries, glassware and ceramic production, tannery operation, dyestuff, pesticide industries, some organic and inorganic chemical manufacturing, petroleum refining, and rare earth metals. As a result both the inorganic and organic arsenic compounds can be found in soil, plants, animals, and humans (1). Arsenic in natural waters is a worldwide problem. Arsenic pollution has been reported recently in the USA, China, Chile, Bangladesh, Taiwan, Mexico, Argentina, Poland, Canada, Hungary, New Zealand, Japan, and India (2). Inorganic arsenic is predominantly present in natural waters. Arsenate [As(V)] and arsenite [As(III)] are primary forms of arsenic in soils and natural waters. As(III) is more mobile in groundwater and 25–60 times more toxic than As(V) (2). The concentration of arsenic species is mainly dependent on redox potentials and pH. Under low pH and mildly reducing conditions, As(III) is thermodynamically stable and exists as arsenious acid ($H_3AsO_3^0$, $H_2AsO_3^-$, $HAsO_3^{2-}$, AsO_3^{3-}) (3). Under oxidizing conditions, the predominant species is As(V) which exists as arsenic acid (H_3AsO_4, $H_2AsO_4^-$, $HAsO_4^{2-}$, AsO_4^3) as stable species in the pH interval 3–6, 7–11, and 12–14 respectively (4,5). Pollution-based studies have shown that arsenate may adversely affect several organs in the human body including cancer of the skin, lung and urinary bladder. United States Environmental Production Agency (USEPA) lowered the maximum concentration level of arsenic in water system to 20 ppb (6). Consequently the removal of arsenic from water system becomes urgent in order to comply with the legislation (7). Conventional methods for removing heavy metal ions include chemical precipitation, chemical oxidation or reduction, filtration, ion exchange, application of membrane technology, and electro dialysis (ED) (8–14). However, these processes have considerable disadvantages including incomplete metal removal, requirements for expensive equipment and monitoring system, high reagent and energy requirements, or the generation of toxic sludge or other waste products that require disposal. During the last few decades electrochemical water treatment technologies have undergone rapid growth

Received 16 September 2009; accepted 8 February 2010.
Address correspondence to Subramanyan Vasudevan, Central Electrochemical Research Institute (CSIR), Karaikudi–630 006, India. Tel.: +91 4565 227556; Fax: +91 4565 227779. E-mail: vasudevan65@gmail.com

and development. One of these technologies is the electrochemically assisted coagulation that can compete with the conventional chemical coagulation process. Electrocoagulation is an emerging water treatment technology that has been applied successfully to treat various wastewaters (15). It has been applied for the treatment of potable water. Further, electrocoagulation offers possibility of anodic oxidation and in situ generation of adsorbents. The electrochemical production of destabilization agents that brings charge neutralization from a pollutant and it has been used for water or wastewater treatment. It has been successfully used to treat oil wastes, with high removal efficiencies as high as 99% (16). Usually magnesium and aluminium plates are used as electrodes in the electrocoagulation followed by the electrosorption process (17–19). The advantages of electrocoagulation include high particulate removal efficiency, a compact treatment facility, relatively low cost, and the possibility of complete automation (20–25). This technique does not require supplementary addition of chemicals and reduces the volume of produced sludge.

(i) When iron is used as a electrode, the reactions are as follows:
At the cathode:

$$2H_2O + 2e^- \rightarrow H_2(g) + 2OH^- \quad (1)$$

At the anode:

$$4Fe(s) \rightarrow 4Fe^{2+}(aq) + 8e^- \quad (2)$$

and with dissolved oxygen in solution:

$$4Fe^{2+}(aq) + 10H_2O(l) + O_2(g) \rightarrow 4Fe(OH)_3 + 8H^+(aq) \quad (3)$$

overall reaction:

$$4Fe(s) + 10H_2O(l) + O_2(g) \rightarrow Fe(OH)_3(s) + 4H_2(g)$$

(ii) When aluminum is used as an electrode, the reactions are as follows:

At the cathode:

$$2H_2O + 2e^- \rightarrow H_2(g) + 2OH^- \quad (4)$$

At the anode:

$$Al \rightarrow Al^{3+} + 3e^- \quad (5)$$

In the solution:

$$Al^{3+}(aq) + 3H_2O \rightarrow Al(OH)_3 + 3H^+(aq) \quad (6)$$

This method is characterized by reduced sludge production, a minimum requirement of chemicals, and ease of operation. Although, there are numerous reports related to electrochemical coagulation as a means of removal of many pollutants from water and wastewater, but there is limited work on arsenic removal by the electrochemical method and its adsorption and kinetics studies. This paper presents the results of the laboratory scale studies on the removal of arsenic using mild steel as both anode and cathode respectively by electrocoagulation process. In doing so, the equilibrium adsorption behavior is analyzed by fitting models of Langmuir, Freundlich, D-R and Frumkin isotherms. Adsorption kinetics of As (V) on $Fe(OH)_3$ is analyzed using first- and second-order kinetic models. Activation energy is evaluated to study the nature of adsorption.

EXPERIMENTAL

Cell Construction and Electrolysis

The electrolytic cell (Fig. 1) consists of a 1.0 – L Plexiglas vessel that was fitted with a polycarbonate cell cover with slots to introduce the anode, cathode, pH sensor, a thermometer and electrolytes. Mild steel with surface area 0.2 dm^2 acted as the anode and cathode of same size were placed at an inter-electrode distance of 0.005 m. Thermodynamic studies were carried out at 313–343 K. The temperature of the electrolyte has been controlled to the desired value with a variation of ± 2 K by adjusting the rate of flow of thermostatically controlled water through an external glass-cooling spiral. A regulated direct current (DC) was supplied from a rectifier (10 A, 0–25 V; Aplab model).

The arsenic as sodium arsenate ($Na_2HAsO_4 \cdot 7H_2O$) (Analar Reagent) was dissolved in deionized water for the required concentration (0.5–1.5 mg L^{-1}). The solution of 0.90 L was used for each experiment as the electrolyte. The pH of the electrolyte was adjusted, if required, with 1 M HCl or 1 M NaOH solutions (AR Grade) before adsorption experiments. To study the effect of co-existing ions, in the removal of As(V), sodium salts (Analar Grade) of phosphate (5–50 mg L^{-1}), silicate (0–15 mg L^{-1}), carbonate (0–250 mg L^{-1}), and fluoride (0–5 mg L^{-1}) was added to the electrolyte.

Analytical Method

Ion Chromatography (Metrohm AG, Switzerland) was used to determine the concentration of arsenate. The SEM of iron hydroxide was analyzed with a Scanning Electron Microscope (SEM) made by Hitachi (model s-3000 h). The XRD of electrocoagulatioan-by products were analyzed by a JEOL X-ray diffractometer (Type – JEOL, Japan). The XPS of the electrocoagulatioan by products were analyzed by a Multilab 2000 (Type – Thermoscientific, UK). The concentration of carbonate, flouride, silicate, and phosphate were determined using UV-Visible Spectrophotometer (MERCK, Pharo 300, Germany).

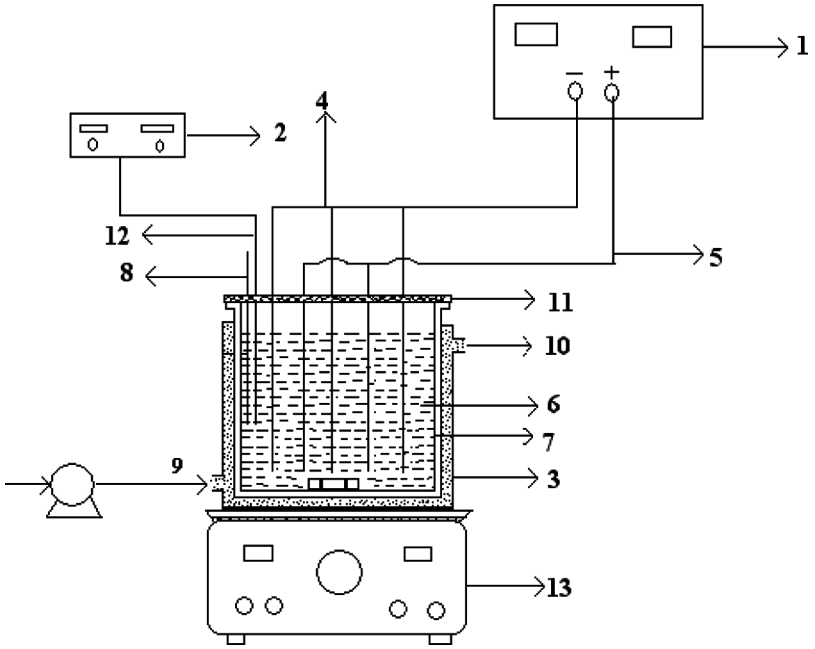

FIG. 1. (1) DC Power Supply, (2) pH meter, (3) Electrochemical cell, (4) Cathodes, (5) Anode, (6) Electrolyte, (7) Outer Jacket, (8) Thermostat, (9) Inlet for thermostatic water, (10) Outlet for Thermostatic water, (11) PVC cover, (12) pH Sensor and (13) Magnetic Stirrer.

RESULT AND DISCUSSION

Effect of Current Density

Among the various operating variables, current density is an important factor which strongly influences the performance of electrocoagulation. The effect of current density on the removal efficiency of AS (V) ions was studied at 0.05, 0.1, 0.2, 0.3, 0.4 A dm^{-2} at an initial concentration of 0.5 mg L^{-1} at pH 7.0. Table 1 illustrates the effect of the current density on the removal efficiency of As (V) which shows that beyond 0.2 A dm^{-2} the removal efficiency remains almost constant for higher current densities. So, further experiments were carried out at 0.2 A dm^{-2}. The results showed that as current density increases, the removal of arsenate also increases. This is due to sufficient current through the solution, the metal ions generated by the dissolution of the sacrificial electrode were hydrolyzed to form a series of metallic hydroxide species. The amount of solubilized iron increases linearly with the current density because of the Faraday law (26). As expected, the amount of arsenate adsorption increases with the increase in adsorbent concentration, which indicates that the adsorption depends upon the availability of binding sites for arsenate.

TABLE 1
Effect of current density for the removal of arsenate from drinking water

Current density (A dm^{-2})	Concentration of arsenate (mg L^{-1})		Removal efficiency (%)
	Initial	Final	
0.05	0.5	0.024	95.2
0.1	0.5	0.016	96.8
0.2	0.5	0.007	98.6
0.3	0.5	0.003	99.4
0.4	0.5	0.002	99.6

Effect of pH

The pH is one of the important factors affecting the performance of the electrochemical process, and to examine this effect, a series of experiments were carried out using 0.5 mg L^{-1} arsenate containing solutions, with an initial pH varying in the range 2 to 12. The removal efficiency of arsenate was increased with increasing the pH up to 7. When the pH is above 7, the removal efficiency should be slightly decreased. It is found that in Fig. 2 the maximum removal efficiency for the removal of arsenate is 98.6% at pH 7 and the minimum efficiency is 95% at pH 2. At acidic and alkaline pHs, the oxide surfaces exhibit net positive and negative charges respectively and would tend to repulse the adsorption of arsenate and resulting in the maximum adsorption at pH 7.

Effect of Initial Arsenate Concentration

In order to evaluate the effect of initial arsenate concentration, experiments were conducted at varying initial

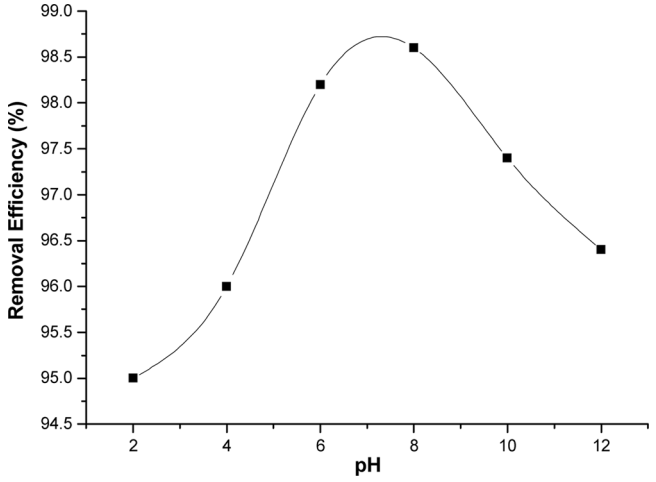

FIG. 2. Effect of pH on the removal of arsenate at a current density of $0.2\,A\,dm^{-2}$, concentration of $0.5\,mg\,L^{-1}$ and temperature of 303 K.

concentration from 0.5–1.5 mg L^{-1}. Figure 3 shows that the uptake of arsenate (mg g^{-1}) increased with an increase in arsenate concentration per gram of $Fe(OH)_3$ and remained nearly constant after equilibrium time. The equilibrium time was found to be 15 min for all concentration studied. The amount of arsenate adsorbed (q_e) increased from 0.451 to 1.483 mg-As g^{-1} as the concentration increased from 0.5–1.5 mg L^{-1}. The amount of adsorbed q_e increases with the increasing concentration of arsenate and reaches a saturation point when the active sites are fully covered with the adsorbate species (27). The plots are single, smooth, and continuous curves leading to saturation, suggesting the possible monolayer coverage to arsenate on the surface of the adsorbent.

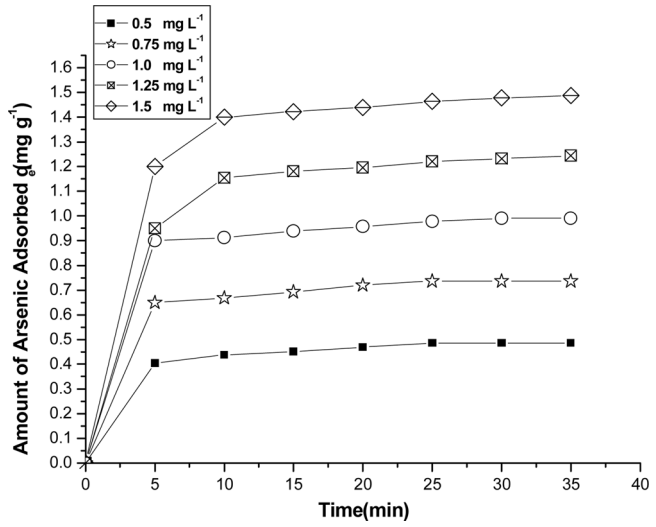

FIG. 3. Effect of agitation time and amount of arsenate adsorbed, at a current density of $0.2\,A\,dm^{-2}$, pH of 7.0, temperature of 303 K.

Adsorption Kinetics

In order to establish the kinetic of arsenate adsorption, the adsorption kinetics of iron anode was investigated by using first-order, second-order kinetic models, Elovich, and intraparticle diffusion.

First-Order Lagergren Model

The first order Lagergren model is generally expressed as follows (28,29),

$$dq_t/dt = k_1(q_e - q_t) \tag{8}$$

where q_e and q_t are the adsorption capacities at equilibrium and at time t (min) respectively, and $k_1(1/min)$ is a rate constant. Equation (8) can be linearized for use in the kinetic analysis of experimental analysis by applying boundary conditions $t = 0$ to $t = t$ and $q_t = 0$ to $q_t = q_t$ as follows,

$$\log(q_e - q_t) = \log(q_e) - k_1 t/2.303 \tag{9}$$

The values of $\log(q_e - q_t)$ were linearly correlated with t. The plot of $\log(q_e - q_t)$ vs t should give the linear relationship from which k_1 and q_e can be determined by the slope and intercept respectively (Fig. 4). Table 2 shows the computed results of first-order kinetics. A large difference of q_e between the experimental and calculated values and low correlation co-efficient values indicates a poor first-order fit for the adsorption kinetics.

Second-Order Lagergren Model

The second order kinetic model is expressed as (30)

$$dq_t/dt = k_2(q_e - q_t)^2 \tag{10}$$

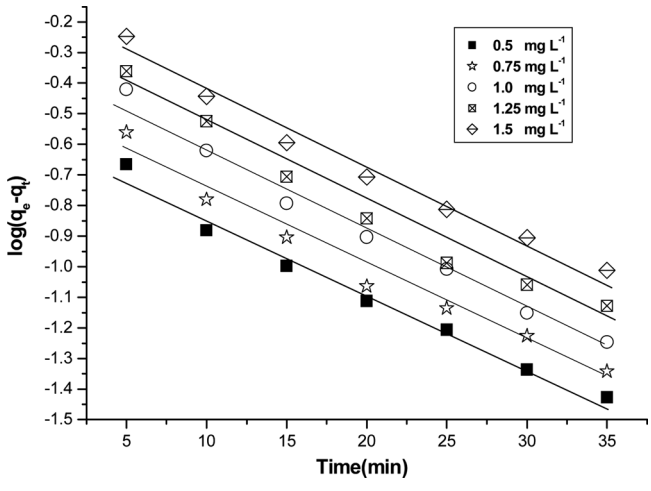

FIG. 4. First order kinetic model plot of different concentrations of arsenate at current density of $0.2\,A\,dm^{-2}$, temperature of 303 K, pH of 7.00.

TABLE 2
Comparison between the experimental and calculated q_e values for different initial arsenate concentrations in first order adsorption isotherm at temperature 305 K and pH 7

Concentration ($mg\,L^{-1}$)	q_e Experimental ($mg\,g^{-1}$)	K_1 ($min\text{-}g\,mg^{-1}$)	q_e Calculated ($mg\,g^{-1}$)	R^2
0.5	0.101	0.151	0.532	0.9724
0.75	0.252	0.136	0.631	0.9528
1.0	0.426	0.089	0.726	0.9955
1.25	0.751	0.072	0.976	0.9536
1.5	0.902	0.065	1.367	0.9662

where k_2 is the rate constant of second-order adsorption. The integrated form of Eq. (10) with the boundary condition $t = 0$ to > 0 ($q = 0$ to > 0) is

$$1/(q_e - q_t) = 1/q_e + k_2 t \tag{11}$$

Equation (11) can be rearranged and linearized as,

$$t/q_t = 1/k_2 q_e^2 + t/q_e \tag{12}$$

The plot of t/q_t and time (t) (Fig. 5) gave a linear relationship from which q_e and k_2 can be determined from the slope and intercept of the plot with high regression co-efficient (Table 3).

Elovich Equation

The Elovich model equation is generally expressed as indicated (31)

$$dq_t/dt = \alpha \exp(-\beta q_t) \tag{13}$$

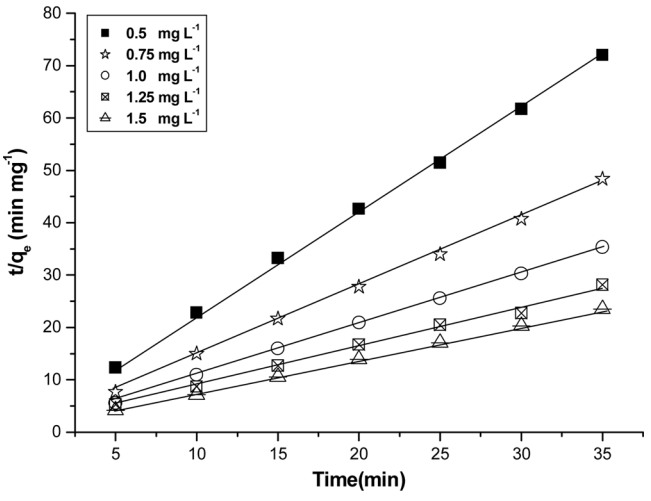

FIG. 5. Second order kinetic model plot of different concentrations of arsenate at current density of 0.2 A dm^{-2}, temperature of 303 K, pH of 7.00.

the simplified form of Elovich Eq. (13) is

$$q_t = 1/\beta \log_e(\alpha\beta) + 1/\beta \log_e(t) \tag{14}$$

where α is the initial adsorption rate ($mg\,g^{-1} \cdot h$) and, β is the desorption constant ($g\,mg^{-1}$). If arsenate adsorption fits the Elovich model, a plot of q_t vs $\log_e(t)$ should yield a linear relationship with the slope of $(1/\beta)$ and an intercept of $1/\beta \log_e(\alpha\,\beta)$. Figure 6 shows values obtained from this model. Table 4 depicts the results obtained from Elovich equation. Lower regression value shows the inapplicability of this model.

IntrA-Particle Diffusion

The Intraparticle Diffusion model is expressed (32,33),

$$R = k_{id}(t)^{\alpha z} \tag{15}$$

A linearized form the Eq. (15) is followed by

$$\log R = \log k_{id} + a \log(t) \tag{16}$$

in which a depicts the adsorption mechanism and k_{id} may be taken as the rate factor (percent of arsenate adsorbed per unit time) (Fig. 7). The higher value of k_{id} illustrates an enhancement in the rate of adsorption, whereas larger k_{id} values illustrate a better adsorption mechanism, which is related to an improved bonding between pollutant and the adsorbent particles.

Tables 2, 3, and 4 depict the computed results obtained from the first-order, second-order, Elovich, and intraparticle diffusion. The correlation coefficient values decreases from second-order, first-order, and intraparticle diffusion to Elovich model. This indicates that the adsorption follows the second-order than the other models. Further, the calculated q_e values well agree with the experimental q_e values for the second-order kinetics model.

Adsorption Isotherm

The adsorption capacity of the $Fe(OH)_3$ coagulant has been tested using the Freundlich, Langmuir,

TABLE 3
Comparison between the experimental and calculated q_e values for different initial arsenate concentrations in second order adsorption isotherm at temperature 305 K and pH **7**

Concentration ($mg\,L^{-1}$)	q_e experimental ($mg\,g^{-1}$)	K_2 ($min\text{-}g\,mg^{-1}$)	q_e calculated ($mg\,g^{-1}$)	R^2
0.5	0.451	0.1286	0.461	0.9992
0.75	0.692	0.0038	0.699	0.9980
1.0	0.939	0.9756	0.953	0.9971
1.25	1.186	0.3881	1.186	0.9994
1.5	1.483	0.5155	1.420	0.9992

Dubinin- Redushkevich, and Frumkin isotherms. These models have been widely used to describe the behavior of the adsorbent-adsorbate couples. To determine the isotherms, the initial pH was kept at 7 and the concentration of arsenate used was in the range of 0.5–1.5 $mg\,L^{-1}$.

Freundlich Isotherm

The general form of Freundlich adsorption isotherm is represented by (34)

$$q_e = KC_e^n \tag{17}$$

Equation (17) can be linearized in logarithmic form and the Freundlich constants can be determined as follows,

$$\log q_e = \log k_f + n\log C_e \tag{18}$$

Where, k_f is the Freundlich constant related to adsorption capacity, n is the energy or intensity of adsorptions and C_e is the equilibrium concentration of arsenate ($mg\,L^{-1}$). The values of k_f and n can be obtained by plotting logarithms of the adsorption capacity against equilibrium concentrations. To determine the isotherms, the arsenate concentration used was 0.5–1.5 $mg\,L^{-1}$ and at an initial pH 7. The Freundlich constants k_f and n values are 0.9444 $mg\,g^{-1}$ and 0.9336 $L\,mg^{-1}$ respectively. It has been reported that the values of n lying between 0 and 10 indicate favorable adsorption. From the analysis of the results it is found that the Freundlich plots fit satisfactorily with the experimental data obtained in the present study (Fig. 8). This is well agreed with the results presented in the literature for adsorption of arsenic (8,35).

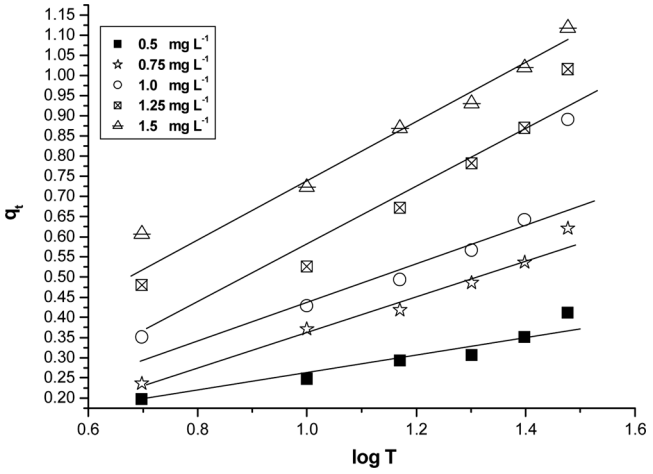

FIG. 6. Elovich model for various concentration of arsenate from 0.5 to 1.5 $mg\,L^{-1}$, current density of 0.2 $A\,dm^{-2}$, temperature of 303 K, pH of 7.00.

Langmuir Isotherm

The linearized form of Langmuir adsorption isotherm model is (36).

$$C_e/q_e = 1/q_o b + C_e/q_o \tag{19}$$

where C_e is the concentration of the arsenate solution ($mg\,L^{-1}$) at equilibrium, q_e the amount of As(V) adsorbed at equilibrium ($mg\,g^{-1}$), q_o is the adsorption capacity (Langmuir constant) and b is the energy of adsorption. Figure 9 shows the Langmuir plot with experimental data. The value of the adsorption capacity q_o as found to be 30.844 $mg\,g^{-1}$, which is higher than that of other commercial and synthetic adsorbents studied (2,37). The lower value of the adsorption capacity of the adsorbent studied

TABLE 4
Elovich model and Intra particle diffusion for different initial arsenate Concentrations at temperature 305 K and pH 7

Elovich model			Intra particle diffusion		
A ($mg\,g^{-1}-h$)	B ($g\,mg^{-1}$)	R^2	k_{id} ($l\,h^{-1}$)	A (%/h)	R^2
13.36	54.38	0.9762	40.28	0.133	0.9914
4.69	39.26	0.9435	36.35	0.165	0.9770
1.26	20.22	0.9332	32.14	0.198	0.9681
1.03	19.34	0.9862	30.26	0.268	0.9763
0.82	12.36	0.9662	28.32	0.339	0.9798

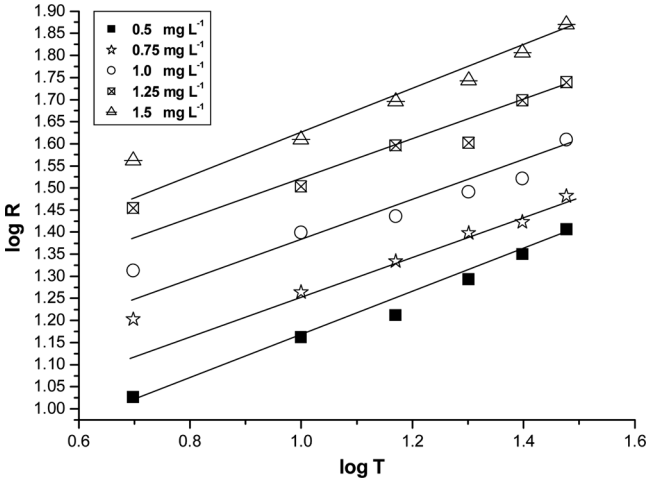

FIG. 7. Intraparticle diffusion model for various concentrations of arsenate from 0.5 to 1.5 mg L^{-1}, current density of 0.2 A dm^{-2}, temperature of 303 K, pH of 7.00.

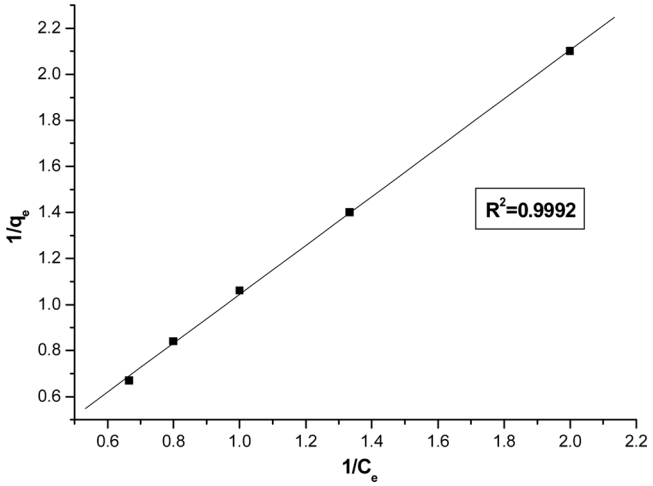

FIG. 9. Langmuir plot for adsorption of arsenate at pH of 7.0, current density of 0.2 A dm^{-2}, temperature of 303 K and concentration of 0.5–1.5 mg L^{-1}.

is due to the pH of the solution, which was found to >7.0. This condition is not favorable for the adsorption of arsenate.

The essential characteristics of the Langmuir isotherm can be expressed as the dimensionless constant R_L,

$$R_L = 1/(1 + bC_o) \tag{20}$$

where R_L is the equilibrium constant it indicates the type of adsorption, b, Co is the Langmuir constant and inition arsenate concentration respectively. The R_L values between 0 and 1 indicate the favorable adsorption. The R_L values were found to be between 0 and 1 for all the concentration of arsenate studied. The results are presented in Table 5.

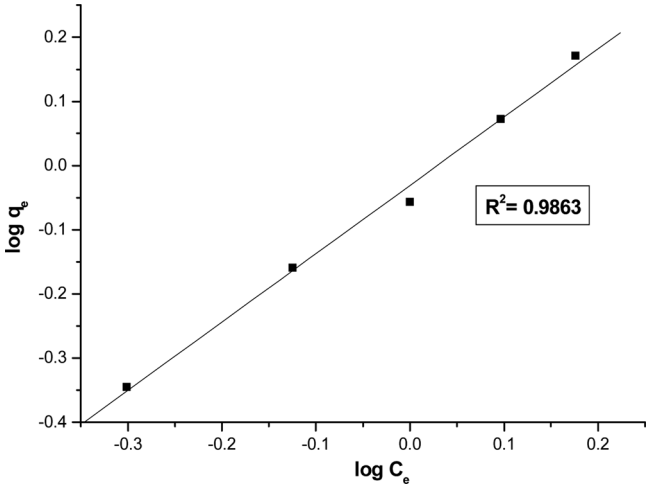

FIG. 8. Freundlich plot for adsorption of arsenate at pH of 7.0, current density of 0.2 A dm^{-2}, temperature of 303 K and concentration of 0.5–1.5 mg L^{-1}.

Dubinin-Radushkevich (D-R) Isotherm

This model is represented by (38),

$$q_e = q_s \exp(-B\varepsilon^2) \tag{21}$$

where $\varepsilon = RT \ln [1 + 1/C_e]$, B is related to the free energy of sorption per mole of the adsorbate as it migrates to the surface of the electrocoagulant ($Fe(OH)_3$) from the infinite distance in the solution and q_s is the Dubinin-Radushkevich (D-R) isotherm constant related to the degree of adsorbate adsorption by the adsorbent surface . The linearized form of the Eq. (21)

$$\ln q_e = \ln q_s - 2BRT \ln[1 + 1/C_e] \tag{22}$$

The isotherm constants of q_s and B are obtained from the intercept and slope of the plot of $\ln q_e$ versus ε^2, (Fig.10) respectively (39). The constant B gives the mean free energy E, of adsorption per molecule of the adsorbate when it is transferred to the surface of the solid from infinity in the solution and the relation is given as

$$E = [1/\sqrt{2B}] \tag{23}$$

The magnitude of E is useful for estimating the type of adsorption process. It was found to be 18.28 kJ mol^{-1}, which is bigger than the energy range of the adsorption reaction, 8–16kJ mol^{-1} (40). So the type of adsorption of As(V) on mild steel was defined as chemical adsorption.

Frumkin Equation

The Frumkin equation indicates the interaction between the adsorbed species. It can be expressed as

$$\theta/(1 - \theta)e^{-2a\theta} = kC_e \tag{24}$$

TABLE 5
Constant parameters and correlation co-efficient calculated for different adsorption models at room temperature for As (V) adsorption

Isotherm	Constants			
Langmuir	$\mathbf{Q_o\ (mg\,g^{-1})}$	$\mathbf{b(L\,mg^{-1})}$	$\mathbf{R_L}$	$\mathbf{R^2}$
	30.844	0.0895	0.9889	0.9992
Freundlich	$\mathbf{K_f\ (mg\,g^{-1})}$	$\mathbf{n\ (L\,mg^{-1})}$		$\mathbf{R^2}$
	0.9444	0.9336		0.9863
D-R	$\mathbf{Q_s\ (\times 10^3\,mol\,g^{-1})}$	$\mathbf{B\ (\times 10^3\,mol^2\,K/J^2)}$	$\mathbf{E\ (KJ\,mol^{-1})}$	$\mathbf{R^2}$
	1.226	1.584	19.22	0.9744
Frumkin	**a**	**lnk**	$\mathbf{-\Delta G\ (KJ\,mol^{-1})}$	$\mathbf{R^2}$
	−0.525	1.705	623.22	0.9439

where $\theta = q_e/q_m$, q_e is the adsorption capacity in equilibrium ($mg\,g^{-1}$), q_m is the theoretical monolayer saturation capacity ($mg\,g^{-1}$). The linearized form is given as

$$\ln[(\theta/(1-\theta))1/C_e] = \ln k + 2a\theta \quad (25)$$

The parameters a and k are obtained from the slope and intercept of the plot ln $[(\theta/(1-\theta))1/C_e]$ Vs θ (Fig. 11). The constant k is related to the adsorption equilibrium.

$$\ln k = -\Delta G/RT \quad (26)$$

The Frumkin equation has been specifically developed to take lateral interaction. The term $e^{-2a\theta}$ in Eq. (24) reflects the extent of lateral interaction, if $a > 0$ indicates attraction, while $a < 0$ means repulsion (41). From Table 5, we see that the value of a is −0.525 indicating the attraction.

The correlation co-efficient values of different isotherm models are listed in Table 5. The regression co-efficient ($R^2 = 0.999$) decreases in the order of Langmuir, Freundlich, D-R, and Frumkin isotherm which shows the better fit to the Langmuir model and also the value of R_L for the Langmuir isotherm was calculated between 0 and 1, indicating the favorable adsorption of arsenate.

Effect of Temperature

The amount of arsenate adsorbed on the adsorbent ($Fe(OH)_3$) increases by increasing the temperature indicating the process to be endothermic. The diffusion co-efficient (D) for the intraparticle transport of arsenate species into the adsorbent particles has been calculated at different temperature by

$$t_{1/2} = 0.03x r_o^2/D \quad (27)$$

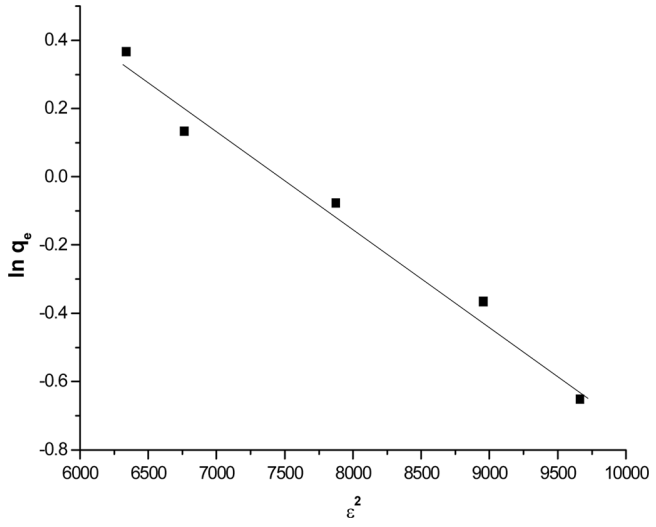

FIG. 10. D-R plot for adsorption of arsenate at pH of 7.0, current density of $0.2\,A\,dm^{-2}$, temperature of 303 K and concentration of 0.5–1.5 $mg\,L^{-1}$.

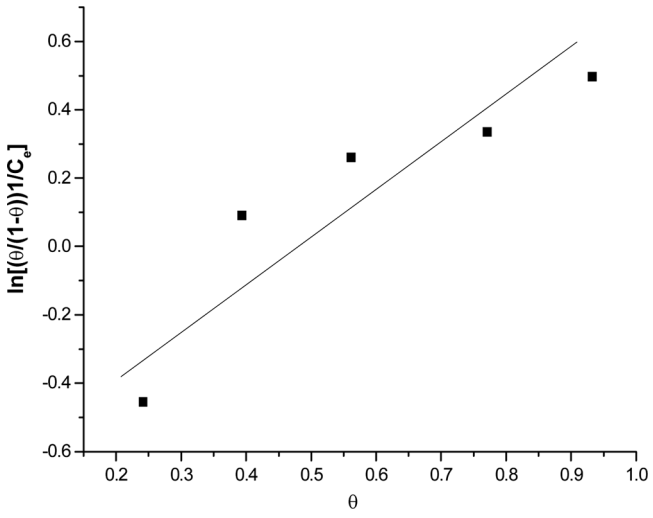

FIG. 11. Frumkin plot for adsorption of arsenate at pH of 7.0, current density of $0.2\,A\,dm^{-2}$, temperature of 303 K and concentration of 0.5–1.5 $mg\,L^{-1}$.

TABLE 6
Pore Diffusion coefficients for the adsorption of arsenate at various temperatures

Temperature (K)	Pore diffusion constant $D \times 10^{-10}$ (cm^2/s)
313	1.553
323	1.265
333	1.004
343	0.923

where $t_{1/2}$ is the time of half adsorption (s), r_o is the radius of the adsorbent particle (cm), and D is the diffusion co-efficient in cm^2/s. For all chemisorption system the diffusivity co-efficient should be 10^{-5} to $10^{-13}\,cm^2/s$ (42). In the present work, D is found to be in the range of $10^{-10}\,cm^2/s$. The pore diffusion coefficient (D) values for various temperatures and different initial concentrations of arsenate are presented in Tables 6 and Table 7 respectively.

To find out the energy of activation for the adsorption of arsenate, the second-order rate constant is expressed in Arhenius form (43).

$$\ln k_2 = \ln k_o - E/RT \tag{28}$$

where k_o is the constant of the equation ($g\,mg^{-1}\cdot min^{-1}$), E is the energy of activation ($J\,mol^{-1}$), R is the gas constant ($8.314\,J\,mol^{-1}\,K$), and T is the temperature in K. Figure 12 shows that the rate constants vary with temperature according to Eqs. (28). The activation energy (18.731 $KJ\,mol^{-1}$) is calculated from the slope of the fitted equation. The free energy change is obtained using the following relationship:

$$\Delta G = -RT\ln K_c \tag{29}$$

where ΔG is the free energy ($KJ\,mol^{-1}$), K_c is the equilibrium constant, R is the gas constant and T is the temperature in K. The K_c and ΔG values are presented in Table 8.

TABLE 7
Pore Diffusion coefficients for the adsorption of arsenate at various concentrations 0.5–1.5 ($mg\,L^{-1}$)

Concentration ($mg\,L^{-1}$)	Pore diffusion constant $D \times 10^{-10}$ (cm^2/s)
0.5	1.263
0.75	1.123
1.0	0.995
1.25	0.869
1.5	0.791

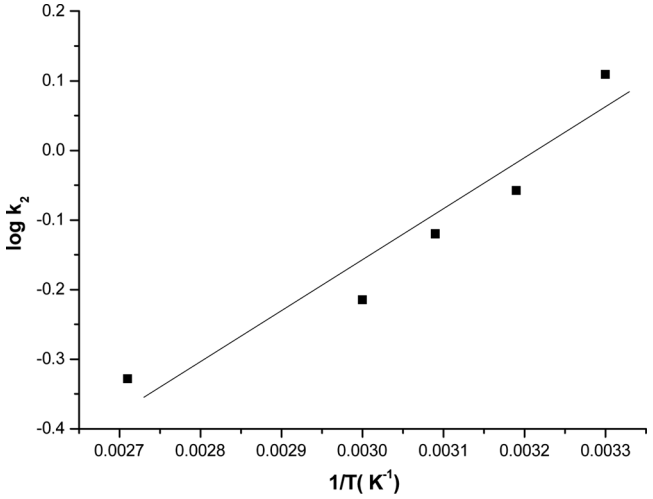

FIG. 12. Plot of log k_2 and 1/T at pH of 7.0, current density of $0.2\,A\,dm^{-2}$, temperature of 303 K and concentration of 0.5–1.5 $mg\,L^{-1}$.

From the table it is found that the negative value of ΔG indicates the spontaneous nature of adsorption.

Other thermodynamic parameters such as entropy change (ΔS) and enthalpy change (ΔH) were determined using van't Hoff equation,

$$\ln kc = \frac{\Delta s}{R} - \frac{\Delta H}{RT} \tag{30}$$

The enthalpy change ($\Delta H = 14.251\,KJ\,mol^{-1}$) and entropy change ($\Delta S = 53.40\,J/mol\cdot K$) were obtained from the slope and intercept of the van't Hoff linear plots of lnKc versus 1/T (Fig. 13). A positive value of enthalpy change (ΔH) indicates that the adsorption process is endothermic in nature, and the negative value of change in internal energy (ΔG) shows the spontaneous adsorption of arsenate on the adsorbent. The positive values of entropy change show the increased randomness of the solution interface during the adsorption of arsenate on the adsorbent shown in Table 8. Enhancement of the adsorption capacity of the electrocoagulant (iron oxide) at higher temperatures may be attributed to the enlargement of pore size and or activation of the adsorbent surface. Using the Lagergran rate

TABLE 8
Thermodynamic parameters for the adsorption of arsenate

Temperature (K)	K_c	ΔG^o ($J\,mol^{-1}$)	ΔH^o ($KJ\,mol^{-1}$)	ΔS^o ($J/mol\,K$)
303	0.0091	−23.266		
313	0.0479	−129.32		
323	0.1276	−397.42	14.251	53.40
333	0.4431	−1283.1		
343	0.6523	−1647.4		

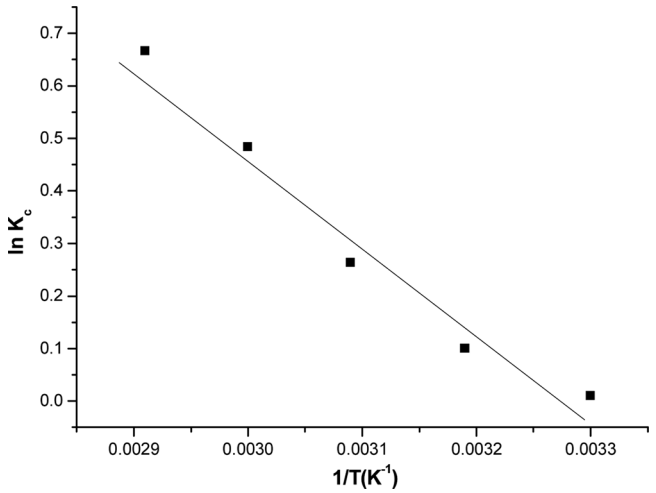

FIG. 13. Plot of log k_c and 1/T at pH of 7.0, current density of 0.2 A dm^{-2}, temperature of 303 K and concentration of 0. 5–1.5 mg L^{-1}.

equation, the first-order rate constants and correlation co-efficient were calculated for different temperatures (305–343 K). The calculated 'q_e' values obtained from the second order kinetics agrees with the experimental 'q_e' values better than the first order kinetics model. Tables 9 and 10 depict the computed results obtained from first- and second-order kinetic models. These results indicate that the adsorption follows the second-order kinetic model at different temperatures used in this study.

Effect of Coexisting Ions

Carbonate

The effect of carbonate on arsenate removal was evaluated by increasing the carbonate concentration from 0 to 250 mg L^{-1} in the electrolyte. The results are presented in Table 11. The arsenate removal efficiencies are 98.6, 98.6, 98.4, 72, 65, 24, and 18% for the carbonate ion concentration of 0, 2, 4, 5, 65, 150, and 250 mg L^{-1} respectively. From the removal efficiency of arsenate, it is found that the removal efficiency of the arsenate is not affected by the presence of carbonate below 5 mg L^{-1}. Significant reduction in removal efficiency was observed at and above 5 mg L^{-1} of carbonate concentration is due to the passivation of anode (hindering the dissolution process).

TABLE 9
Comparison between the experimental and calculated q_e values for Initial arsenate concentration 0.5 mg L^{-1} in First order adsorption isotherm at various temperatures

Temperature (K)	q_e experimental (mg g^{-1})	K_1 min-g mg^{-1}	q_e calculated (mg g^{-1})	R^2
313	0.101	0.151	0.532	0.9762
323	0.092	0.146	0.332	0.9645
333	0.086	0.143	0.139	0.9668
343	0.077	0.139	0.103	0.9865

TABLE 10
Comparison between the experimental and calculated q_e values for Initial arsenate concentration 0.5 mg L^{-1} in second order adsorption isotherm at various temperatures (pH 7)

Temperature (K)	q_e experimental (mg g^{-1})	K_2 min-g mg^{-1}	q_e calculated (mg g^{-1})	R^2
313	0.438	0.126	0.421	0.9992
323	0.441	0.132	0.439	0.9982
333	0.446	0.136	0.441	0.9898
343	0.451	0.141	0.448	0.9988

TABLE 11
Effect of addition of carbonate, phosphate, silicate and fluoride in the electrolyte for the removal of arsenate from water

Concentration (mg L^{-1})	Voltage (V)	Concentration of arsenate (mg L^{-1})		Removal efficiency of Arsenate (%)
		Initial	Final	
Carbonate				
0	1.5	0.5	0.007	98.6
2.0	1.5	0.5	0.007	98.6
4.0	1.5	0.5	0.008	98.4
5.0	1.8	0.5	0.14	72.0
65.0	2.0	0.5	0.17	65.0
150.0	2.2	0.5	0.38	24.0
250.0	2.7	0.5	0.41	18.0
Phosphate				
0	1.5	0.5	0.007	98.6
2.0	1.8	0.5	0.008	98.4
4.0	1.8	0.5	0.008	98.4
5.0	1.8	0.5	0.18	64.0
25.0	2.0	0.5	0.25	50.0
50.0	2.6	0.5	0.28	45.0
Silicate				
0	1.5	0.5	0.007	98.6
5.0	1.8	0.5	0.20	60.0
10.0	2.3	0.5	0.30	48.0
15.0	2.6	0.5	0.38	27.0
Fluoride				
0	1.5	0.5	0.007	98.6
0.2	1.5	0.5	0.07	86.0
0.5	1.5	0.5	0.17	66.0
2.0	1.9	0.5	0.30	48.0
5.0	2.0	0.5	0.40	20.0

Phosphate

The concentration of phosphate ion was increased from 0 to 50 mg L^{-1}, the contaminant range of phosphate in the ground water. The removal efficiency for arsenate was 98.6, 98.4, 98.4, 64, 50 and 45% for 0, 2, 4, 5, 25, and 50 mg L^{-1} of phosphate ion respectively. The results are presented in Table 11. There is no change in the removal efficiency of arsenate below 5 mg L^{-1} of phosphate in the water. At higher concentrations (at and above 5 mg L^{-1}) of phosphate, the removal efficiency decreases to 45%. This is due to the preferential adsorption of phosphate over arsenate as the concentration of phosphate increase.

Silicate

The effect of silicate on the removal efficiency of arsenate is presented in Table 11. The respective efficiencies for 0, 5, 10 and 15 mg L^{-1} of silicate are 98.6, 60, 48, and 24%. The removal of arsenate decreased with increasing silicate concentration from 0 to 15 mg L^{-1}. In addition to preferential adsorption, it is observed that the silicate can interact with iron hydroxide to form soluble and highly dispersed colloids that are not removed by normal filtration.

Fluoride

From the results it is found that the efficiency decreased from 98.6 to 20% by increasing the concentration of fluoride from 0 to 5 mg L^{-1}. The results on the removal efficiency of arsenate are presented in Table 11. Like phosphate ion, this is due to the preferential adsorption of fluoride over arsenate as the concentration of fluoride increases. So, when fluoride ions are present in the water to be treated, fluoride ions compete greatly with arsenate ions for the binding sites.

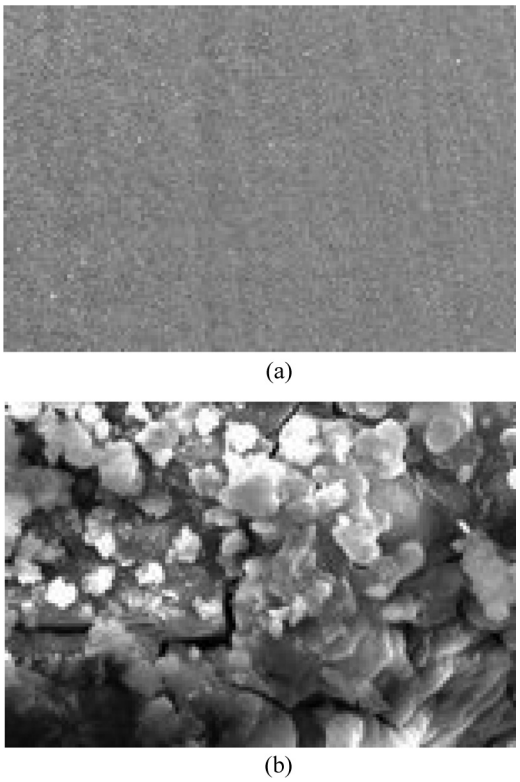

FIG. 14. SEM images (at 1.0k) of the mild steel anode (a) before, (b) after treatment.

Coagulant Characterization

SEM

SEM images of mild steel anode, before and after, electrocoagulation of arsenate electrolyte was obtained to compare the surface texture. Figure 14(a) shows the original mild steel anode plate surface prior to its use in electrocoagulation experiments. The surface of the electrode is uniform. Figure 14(b) shows the SEM of the same electrode after several cycles of use in the electrocoagulation experiments. The electrode surface is now found to be rough, with a number of dents of ca. 1.0 mm. These dents are formed around the nucleus of the active sites where the electrode dissolution results in the production of iron hydroxides. The formation of a large number of dents may be attributed to the anode material consumption at active sites due to the generation of oxygen at its surface.

XPS Studies

The oxidation state of the arsenate in the coagulant was determined using XPS. It is reported that arsenate, As(V), has a 3d binding energy of 45.5 eV. From the XPS spectra (Fig. 15) it is found that the As(V) treated coagulant exhibited a peak at 45.5 eV. The peak position was in close agreement with As(V) 3d binding energy reported in the literature (44).

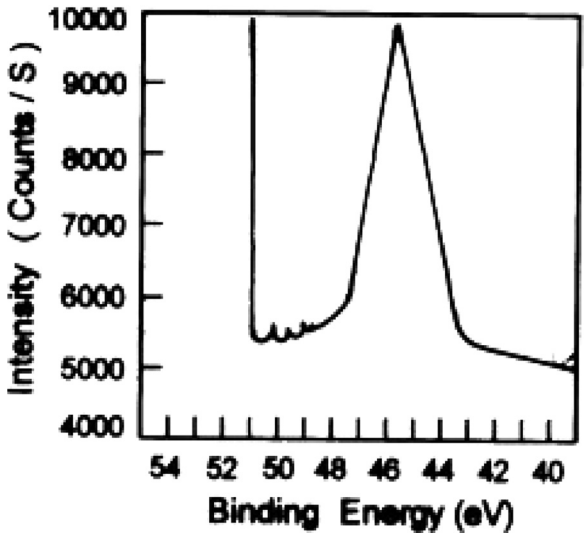

FIG. 15. **XPS** spectrum of arsenate -adsorbed iron hydroxide.

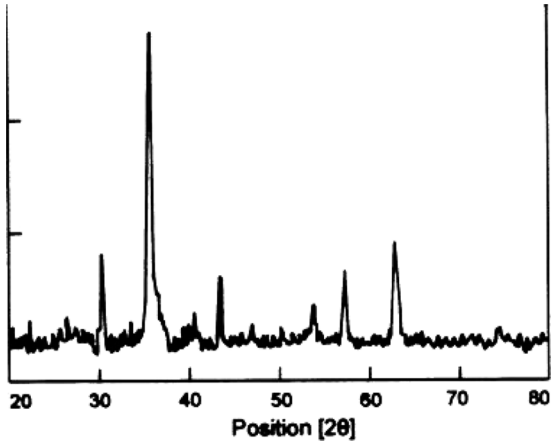

FIG. 16. XRD spectrum of arsenic -adsorbed iron hydroxide.

XRD Studies

The electrocoagulation by-product showed the well crystalline phase such as iron oxide hydroxide (43.3743), magnetite (maximum at 40.6746), and iron hydrogen arsenate at 43.3743 eV (Fig. 16).

CONCLUSION

The results showed that the optimized removal efficiency of 98.6% was achieved at a current density of 0.2A dm^{-2} and pH of 7.0 using mild steel as both anode and cathode. The iron hydroxide generated in the cell remove the arsenate present in the water and to reduce the arsenate concentration to 0.01 mg L^{-1}, and made it for drinking. The adsorption of arsenate on $Fe(OH)_3$ preferably fitting the Langmuir adsorption isotherm. The adsorption process follows-second-order kinetics. Temperature studies showed that adsorption was endothermic and spontaneous in nature.

ACKNOWLEDGEMENTS

The authors wish to express their gratitude to the Director, Central Electrochemical Research Institute, Karaikudi for publishing this paper.

REFERENCES

1. Zhang, F.S.; Itoh, H. (2005) Iron oxide loaded slag for arsenic removal from aqueous systems. *Chemosphere*, 60: 319–325.
2. Mohan, D.; Pittman Jr, C.U. (2007) Arsenic removal from water/wastewater using adsorbents–A critical review. *J. Hazard. Mater.*, 142: 1–53.
3. Altundogan, H.S.; Altundogan, S.; Tumen, F.; Bildik, M. (2002) Arsenic adsorption from aqueous solutions by activated red mud. *Waste Manage.*, 22: 357–363.
4. Manning, A.; Fendorf, E.; Goldberg, S. (1998) Surface Structure and stability of Arsenic (III) on goethite: Spectroscopic evidence for inner sphere complexes. *Environ. Sci. Technol.*, 32: 2383–2388.
5. Stanic, T.; Dakavic, A.; Zivanovic, A.; Canovic, M.; Vera Dondur.; Milicevic, S. (2008) Adsorption of Arsenic (V) by iron modified natural zeolitic tuff. *Environ. Chem. Let.*, 7: 161–166.
6. USEPA (2001) National primary drinking water regulations; arsenic and clarification to contaminants monitoring. 66: 6975–7066.
7. Dousava, B.; Machovic, V.; Kolousek, D.; Kovanda, F.; Dornicak, V. (2003) Sorption of As(V) species from aqueous systems. *Water, Air, Soil Pollut.*, 49: 251–269.
8. Namashivayam, C.; Senthilkumar, S. (1998) Removal of arsenic (V) from aqueous solution using industrial solid waste: adsorption rates and equilibrium studies. *Ind. Eng. Chem. Res.*, 37: 4816–4822.
9. Seko, N.; Basuki, F.; Tamada, M.; Yoshii, F. (2004) Rapid removal of arsenic (V) by irconium (IV) loaded phosphoric chelate adsorbent synthesized by radiation induced graft polymerization. *React. Funct. Polym.*, 59: 235–241.
10. Zeng, L. (2004) A method for preparing silica-containing iron(III) oxide adsorbents for arsenic removal. *Water Res.*, 37: 4351–4358.
11. Emett, M.T.; Khoe, G.H. (2001) Photochemical oxidation of arsenic by oxygen and iron in acid solution. *Water Res.*, 35: 649–656.
12. Fendorf, S.M.; Eick, J.; Grossl, P.R.; Sparks, D.L. (1997) Arsenate and chromate retention mechanisms on goethite surface structure. *Environ. Sci. Tech.*, 31: 315–320.
13. Zhang, Y.; Yang, M.; Huang, X. (2003) Arsenic (V) removal with a Ce(IV)-doped iron oxide adsorbent. *Chemosphere*, 51: 945–952.
14. Xu, Y.H.; Nakajima, T.; Ohki, A. (2002) Adsorption and removal of arsenic (V) from drinking water by aluminium- loaded shirasu-zeolite. *J. Hazard. Mater.*, B92: 275–287.
15. Ratna kumar, P.; Sanjeev, C.; Khilar, C.; Mahajan, S.P. (2004) Removal of arsenic from water by electrocoagulation. *Chemosphere*, 55: 1245–1252.
16. Xu, X.; Zhu, X. (2004) Treatment of refectory oily wastewater by electro-coagulation process. *Chemosphere*, 56: 889–894.
17. Chen, X.; Chen, G.; Yue, P.L. (2002) Investigation on the electrolysis voltage of electrocoagulation. *Chem. Eng. Sci.*, 57: 2449–2455.
18. Chen, G. (2004) Electrochemical technologies in wastewater treatment. *Sep. Purif. Technol.*, 38: 11–41.
19. Adhoum, N.; Monser, L. (2004) Decolourization and removal of phenolic compounds from olive mill wastewater by electrocoagulation. *Chem. Eng. Process*, 43: 1281–1287.
20. Rajeshwar, K.; Ibanez, J.K. (1997) *Environmental Electrochemistry: Fundamentals and Applications in Pollution Abatement*; Academic Press: San Diego.
21. Vik, E.A.; Carlson, D.A.; Eikum, A.S.; Gjessing, E.T. (1984) Electroocoagulation of potable water. *Water Res.*, 18: 1355–1360.
22. Onder, E.; Koparal, A.S.; Ogutveren, U.B. (2007) An alternative method for the removal of surfactants from water: Electrochemical coagulation. *Sep. Purif. Technol.*, 52: 527–532.
23. Ikematsu, M.; Kaneda, K.; Iseki, M.; Yasuda, M. (2007) Electrochemical treatment of human urine for its storage and reuse as flush water. *Sci. Total Environ.*, 382: 159–164.
24. Christensen, P.A.; Egerton, T.A.; Lin, W.F.; Meynet, P.; Shaoa, Z.G.; Wright, N.G. (2006) A novel electrochemical device for the disinfection of fluids by OH radicals. *Chem. Commun.*, 38: 4022–4023.
25. Carlos, A.; Huitle, M.; Ferro, S. (2006) Electrochemical oxidation of organic pollutants for the wastewater treatment: direct and indirect processes. *Chem. Soc. Rev.*, 35: 1324–1340.
26. Vasudevan, S.; Lakshmi, J.; Sozhan, G. (2009) Studies on the removal of iron from drinking water by electrocoagulation – A clean process. *Clean*, 37: 45–51.
27. Manna, B.R.; Debnath, S.; Hossain, J.; Ghosh, U.C. (2004) Trace arsenic contaminated groundwater upgradation using hydrated zirconium oxide (HZO). *J. Indus. Pollut. Cont.*, 20: 247–266.
28. Manna, B.; Ghosh, U.C. (2007). Adsorption of arsenic from aqueous solution on synthetic hydrous stannic oxide. *J. Hazard. Mater.*, 144: 522–531.
29. Raven, K.P.; Jain, A.; Loeppert, R.H. (1998) Arsenite and arsenate adsorptiom on ferrihydride: kinetics, equilibrium and adsorption envelopes. *Environ. Sci. Tech.*, 32: 344–349.

30. Erhan, D.; Kobya, M.; Elif, S.; Ozkan, T. (2004) Adsorption kinetics for the removal of chromium III from aqueous solutions on the activated carbonaceous prepared from agricultural wastes. *Water SA.*, 30: 533–540.
31. Oke, I.A.; Olarinoye, N.O.; Adewusi, S.R.A. (2008) Adsorption kinetics for arsenic removal from aqueous solutions by untreated powdered eggshell. *Adsorption*, 14: 85–92.
32. Weber Jr, W.J.; Morris, J.C. (1963) Kinetics of adsorption on carbon from solutions. *J. Sanit. Div. Am. Soc. Civ. Eng.*, 89: 31–59.
33. Allen, S.J.; Mckay, G.; Khader, K.H.Y. (1989) Intraparticle diffusion of basic dye during adsorption onto sphagnum peat. *Environ. Pollut.*, 56: 39–50.
34. Gasser, M.S.; Morad, G.H.A.; Aly, H.F. (2007) Batch kinetics and thermodynamics of Cr ions removal from waste solutions using synthetic adsorbents. *J. Hazard. Mater.*, 142: 118–129.
35. Jaroniec, M. (1983) Current state in adsorption from multicomponent solutions of nonelectrolytes on solids. *Adv. Colloid Interface Sci.*, 18: 149–225.
36. Manna, B.R.; Dasgupta, M.; Ghosh, U.C. (2004) Studies on crystalline hydrous titanium oxide (CHTO) as scavenger of arsenic (III) from natural water. *Water SRT-AQUA.*, 53: 483–495.
37. Ho, Y.S.; McKay, G. (1999) The sorption of lead (II) ions on peat. *Water Res.*, 33: 578–584.
38. Tan, I.A.W.; Hameed, B.H.; Ahmed, A.L. (2007) Equilibrium and kinetics studies on the basic dye adsorption by palm fibre activated carbon. *Chem. Eng. J.*, 127: 111–119.
39. Demiral, H.; Demiral, I.; Tumsek, F.; Karacbacakoglu, B. (2008) Adsorption of Chromium (Vl) from aqueous solution by activated solution by activated carbon derived from olive bagasse and applicability of different adsorption models. *Chem. Eng. J.*, 144: 184–188.
40. Oguz, E. (2005) Adsorption characteristics and the kinetics of the Cr(VI) on the thuja oriantalis. *Colloid Surf. A*, 252: 121–128.
41. Lazaridis, N.K.; Bakayannakis, D.N.; Deliayanni, E.A. (2005) Chromium(VI) sorptive removal from aqueous solutions by nanocrystalline akaganeite. *Chemosphere*, 58: 65–73.
42. Yang, X.Y.; Al-Duri, B. (2001) Application of branched pore diffusion model in the adsorption of reactive dyes on activated carbon. *Chem. Eng. J.*, 83: 15–23.
43. Golder, A.K.; Samantha, A.N.; Ray, S. (2006) Removal of phosphate from aqueous solution using calcined metal hydroxides sludge waste generated from electrocoagulation. *Sep. Purif. Technol.*, 52: 102–109.
44. Bang, S.; Johnson, D.M.; Korfiatis, P.G.; Meng, X. (2005) Chemical reactions between arsenic and zero-valent iron in water. *Water Res.*, 39: 763–770.